Available online at www.sciencedirect.com
ScienceDirect
Journal of the European Ceramic Society 30 (2010) 1897–1901
www.elsevier.com/locate/jeurceramsoc

Positron annihilation spectroscopic study of hydrothemally synthesized fine nanoporous hydroxyapatite agglomerates

R. Morsy [a,*], M. Elsayed [b], R. Krause-Rehberg [b], G. Dlubek [c], T. Elnimr [a]

[a] *Biophysics Lab, Faculty of Science, Tanta University, Elbahr, Tanta 31527, Egypt*
[b] *Deptartment of Physics, University Halle, D-06099 Halle, Germany*
[c] *ITA Institut für Innovative Technologien, Wiesenring 4, D-06120 Halle, Germany*

Received 1 December 2009; received in revised form 16 February 2010; accepted 16 March 2010

Abstract

Nanoporous hydroxyapatite ($Ca_{10}(PO4)_6(OH)_2$) powders in the form of agglomerates with micrometer dimension were synthesized through hydrothermal wet chemical route. The fine agglomerates were characterized by X-ray diffraction, infrared spectroscopy, scanning electron microscopy and transmission electron microscopy (TEM). Here we use positron annihilation lifetime spectroscopy (PALS) to indicate significant nanoporosity of agglomerates. The longest lifetime component τ_4, which is ascribed to the annihilation of ortho-positronium (o-Ps) localized at mesopores, provides information about the pore size. τ_4 varied at 300 K between 93 and 111 ns. The mean size of mesopores D is determined to vary between 6.8 and 11.6 nm. The spectra were also analyzed allowing a size distribution.

Keywords: Bioceramics; Hydroxyapatite; Agglomeration; Porosity; Positron annihilation lifetime

1. Introduction

Hydroxyapatite (HAp) $Ca_{10}(PO4)_6(OH)_2$ is attracting interest as one of the most active phosphate bioceramics.[1] One of the methods for producing HAp powder is using hydrothermal wet chemical techniques.[2] The precipitation of HAp from solutions is a nucleation–agglomeration growth process.[3] Agglomeration of nanoparticle systems during wet chemical techniques is a nature phenomenon due to adhesion of nanoparticles to each other under attraction of weak van der Waals and capillary adhesive.[4,5] Agglomeration of particles in the smallest size interval makes them visible where it is not possible to distinguish in crystallization process between nuclei of different sizes due to insufficient resolutions of measuring devices in this range of small particle sizes.[6] Agglomeration of nanoparticles is the main problems encountered in preparation of powders by wet chemical methods where agglomeration strongly affects material performance by changing the high surface energy and chemical activity of nanoparticles.[7,8] The parameters governing the macroscopic behavior of the agglomerates are poorly understood at present and their relationships with the properties of the primary particles, the nature of the inter-particle bond and the structure of the agglomerates are not well established.[9] Pore size and pore size distribution of porous ceramic in nanometer range are determined by conventional intrusive techniques such as Hg intrusion porosimetry, adsorption porosimetry (N_2 or CO_2)[10] and electron microscopic investigations. However, commonly they have one problem: their sensibility is limited to at a pore size smaller than 10 nm.[11] Nowadays, it is important to characteristic the pore structure of HAp agglomerates with accuracy and precision technique such as positron annihilation lifetime spectroscopy (PALS).[12] PALS is known to be a very powerful experimental method for studying on a sub-nanometer scale the size of local free volumes.[13,14] It has been used to probe the pore characteristics (size and distribution) in mesoporous systems and in polymers. The technique is sensitive to all pores (both interconnected and closed) in the size range from 0.3 to 300 nm, even in films buried under a diffusion barrier.[15] PALS may be particularly useful in deducing the pore size distribution in closed-pore systems where gas absorption methods are not available. It allows a non-destructive measurement. In dielectric amorphous material a part of the positrons is often formed

* Corresponding author. Tel.: +20 402443076.
E-mail address: Reda_Morsy_Biophysics@yahoo.com (R. Morsy).

0955-2219/$ – see front matter © 2010 Elsevier Ltd. All rights reserved.
doi:10.1016/j.jeurceramsoc.2010.03.014

to a bound state of a positron and an electron which is called positronium (Ps).[16] The electron density in matter must be sufficiently low in order to allow the formation of positronium. Para-positronium has a very short self-annihilation lifetime of $\tau = 0.125$ ns and is not suitable to deliver information about the pore size. It annihilates intrinsically (i.e. annihilation between the particles forming the Ps) mainly into two γ-rays of 511 keV. However, ortho-positronium annihilates in vacuum into three γ-rays in order to conserve spin. In matter, the positron wave function overlaps with electrons outside the positronium. The long vacuum lifetime of the o-Ps of $\tau = 142$ ns is, however, an adequate sensor for measuring the pore size. The vacuum lifetime of o-Ps can be reduced markedly by pick-off annihilation (interaction with electrons of the host material). The reduced Ps lifetime is, therefore, correlated with pore size and is the key feature in transforming a Ps lifetime distribution into a pore size distribution. So information about the pore size can be obtained from the annihilation lifetime which can be extracted by utilizing approved models like the Tao–Eldrup model[17,18] for pore sizes smaller than 1 nm and the Tokyo model[19] or RTE model[11] for larger pore sizes. To obtain proper results when measuring porous systems one must take into consideration the activity of the used positron source because of the comparatively weak intensity of the long lifetime component. When using too strong positron sources the long lifetime component is completely overlapped with the background and a correct analysis of the spectra is not possible.[20]

In this work, we demonstrated that PALS can be used as a unique invasive technique combined with X-ray diffraction (XRD), scanning electron microscope (SEM) techniques to obtain a consistent picture of porous structures in fine HAp agglomerates.

2. Experimental method

Agglomerates of calcium hydroxyapatite were synthesized by co-precipitation using $Ca(OH)_2$ and H_3PO_4 (Adwic, El-nasr Chemical Co., Cairo, Egypt) as starting materials. Three hundred millilitres of a suspension containing 0.5 mole of calcium hydroxide was prepared by adding the powders to distilled water using a stirrer. Three hundred millilitres of a solution contains 0.3 mole of phosphoric acid (85.0–87.0%) H_3PO_4. The H_3PO_4 aqueous was slowly added to the $Ca(OH)_2$ suspension at a rate of 4–5 ml min^{-1} until the Ca/P molar ratio reached 1.667. The reaction mixtures were stirred during the precipitation process, which proceeded at 70 °C. The resulting HAp slurry was allowed to boil for 1 h. The product was transfer to a stainless steel autoclave and the temperature was raised to 130 °C, whereupon a pressure of 1.5 bar was established. The mixture was heated under these conditions for a variable time from 0 to 5 h drying the slurry mixture was carried out by a spray drier. The slurry was extracted from a tank and passed through the spray nozzle. The automized liquid drops were dried rapidly by falling out on hot plate of Teflon that was preheated at 250 °C. Before and after the hydrothermal treatment in the autoclave at 130 °C for 1–5 h, HAp agglomerates were characterized by XRD and scanning electron microscopy. The crystalline structure and particle size of all HAp samples were characterized by X-ray powder diffraction (XRD) using a Philips PW 1840 diffractometer (Eindhoven, Netherlands) with CuK_α radiation. The microstructures of the HAp agglomerates were examined by scanning electron microscopy (SEM) using a JEOL 6400 electron microscope (JEOL Ltd., Tokyo, Japan) and transmission electron microscopy (TEM) images were recorded on a JEM 100SX (JEOL, Co., Japan) operating at an acceleration voltage of 80 kV. The PALS measurements were performed using a fast-fast coincidence system with a time resolution of 260 ps (FWHM).[21] Na_2CO_3 is covered by a 3 μm thick aluminum foil on each side of the source. Spectra with a total count number of 5×106 were recorded. The activity of the used positron source was 0.18 MBq (∼5.0 μCi). Such a weak source is required to obtain the long lifetime component τ_4 in a sufficient way. The measurements were done under ultra high vacuum. Each measurement lasted 6–7 days leading to a lifetime spectrum of 5.3×106 coincidence counts. This high statistics is necessary when analyzing the lifetime spectra with the routine LT9.0 in its distribution mode.[21] The source correction of 13% (Al foil) and the time resolution were determined by measuring a n-type silicon reference sample, showing no positron traps. The final resolution function used in the spectrum analysis was determined as the sum of two Gaussians.

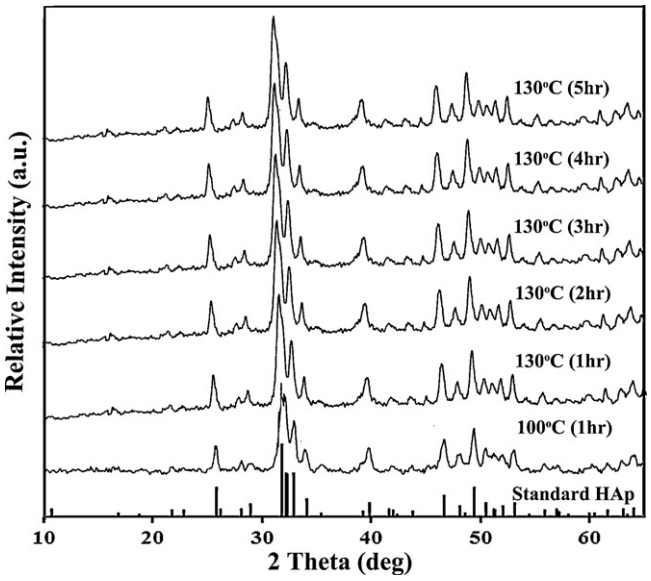

Fig. 1. X-ray diffraction patterns of HAp agglomerates at various reaction times compared with the JCPDF file 9–432 of standard HAp.

3. Results and discussions

XRD patterns of HAp samples have been compared with JCPDS standard HAp card which has been used for X-ray phase identification.[22] Fig. 1 shows XRD patterns of standard HAp and our prepared HAp before and after hydrothermal treatment in the autoclave for 1–5 h. All peaks of HAp samples correspond to the standard pure HAp reflections and indicate single phase structure, with a strong (2 1 1) peak at 2θ—31.7°. XRD patterns characteristics of HAp samples do not show changes

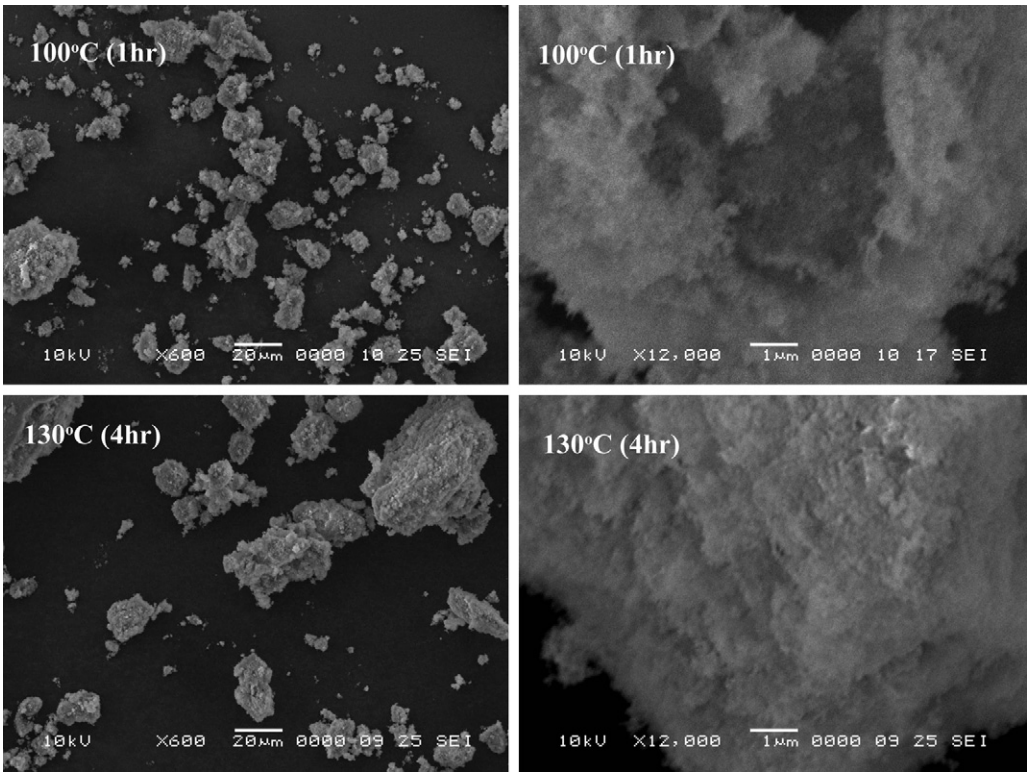

Fig. 2. SEM micrographs of HAp agglomerates at reaction times 1 and 4 h.

with increasing time from 1 to 5 h, HAp peaks have the same sharpness and width.

In order to study the effect of reaction time on the crystallite size of the HAp samples, the Scherrer equation was used [20], Eq. (1):

$$t = \frac{0.9\ \lambda}{B \cos \theta_B} \quad (1)$$

where t is the mean crystallite size, B is the peak line-width at half maximum (in radian), θ_B is the Bragg diffraction angle and λ is the X-ray wavelength. The (0 0 2) peak reflection at 2θ—25.9° was chosen for analysis of the broadening of the Bragg line. The results indicate that the crystallite size of all HAp agglomerates has a value at about 7 nm indicating that the crystallite size of the HAp agglomerates is not responding to the extent with reaction time.

The SEM images of all resulting HAp agglomerates for various reaction times are given in Fig. 2. It is clear that the agglomerates of HAp particles have three-dimensional structures with irregular shapes and non-uniform sizes. The initial fine HAp agglomerates consists of primary particles of size less than 20 μm. At first glance, SEM images of a magnification at 12,000 or more show that the HAp agglomerates reveal appearance of snowflakes rather than obvious ordered crystalline structure.[9,23] It is difficult to observe the particles size or void spaces between the joined HAp particles by SEM due to insufficient resolutions of measuring devices in this range of small particle sizes.[6]

The TEM image of all resulting HAp agglomerates is given in Fig. 3. TEM image of HAp agglomerates at high magnification shows that the HAp particles reveal high agglomeration

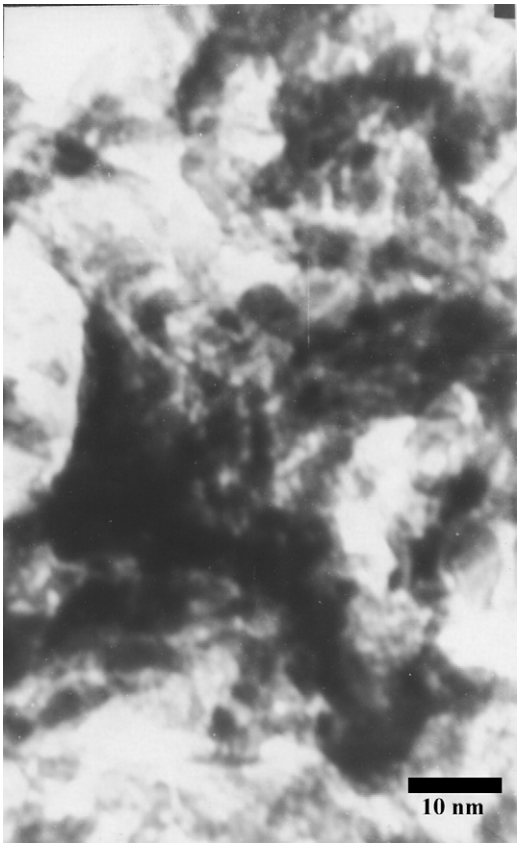

Fig. 3. TEM micrographs of HAp agglomerates.

Table 1
Lifetimes and intensities of positron annihilation of investigated HAp samples. The o-Ps lifetime τ_4 corresponds to the size of the mesopores.

Samples	τ_2 (ns)	τ_3 (ns)	τ_4 (ns)	I_2 (%)	I_3 (%)	I_4 (%)
1	0.390 ± 4.6E−4	3.0 ± 0.02	97.6 ± 0.8	82.7 ± 0.1	4.1 ± 0.03	6.1 ± 0.03
2	0.401 ± 7.7E−4	3.7 ± 0.03	93.1 ± 0.7	82.9 ± 0.2	4.4 ± 0.03	5.8 ± 0.03
3	0.380 ± 5.3E−4	2.3 ± 0.02	103.3 ± 0.7	84.8 ± 0.1	4.0 ± 0.04	5.7 ± 0.02
4	0.375 ± 7.9E−4	2.6 ± 0.01	106.4 ± 0.7	79.8 ± 0.2	3.8 ± 0.03	4.9 ± 0.03
5	0.375 ± 6.0E−4	2.8 ± 0.01	102.5 ± 0.6	78.5 ± 0.2	3.6 ± 0.02	4.7 ± 0.02
6	0.360 ± 6.1E−4	2.1 ± 0.01	111.0 ± 0.5	81.9 ± 0.1	3.7 ± 0.02	4.7 ± 0.01

with void spaces between the joined HAp particles rather than obvious individual particles.

HAp samples (1–6) were investigated by positron lifetime spectroscopy. All the samples are boiled at 100 °C for 1 h. The samples (2–6) are treated by an autoclave at 130 °C for 1, 2, 3, 4 and 5 h respectively. Only sample 1 is not treated at 130 °C.

All lifetime spectra of the samples consist of four different lifetime components which have its origin in the annihilation of the p-Ps ($\tau_1 = 0.125$ ns), the annihilation of free positrons (τ_2), the annihilation of o-Ps in the amorphous region due to the structural disorder (τ_3) and the annihilation of o-Ps in the larger mesopores (τ_4). For analysis of the spectra, the routine LT version 9.0 was used. In the fitting routine the background was a free parameter.

LT9.0 assumes that the distribution function of the annihilation rate λ ($\lambda = 1/\tau$) of each decay channel i, $\alpha i(\lambda)$, follow a logarithmic Gaussian function. In the final fits we assumed that the (very short) p-Ps lifetime and (very large) o-Ps lifetime appear discrete (standard deviation of lifetime distribution σ_1, $\sigma_4 = 0$), while the positron and lower o-Ps lifetimes were allowed to show a distribution (σ_2, $\sigma_3 > 0$). Moreover, to reduce the scatter of fitted parameters, we fixed the p-Ps lifetime to its average from unconstrained fits, $\tau_1 = 0.125$ ns. A typical positron lifetime spectrum of one of the samples is shown in Fig. 4, as example. As shown, the spectrum consists of four different exponential lifetime components. The longest lifetime component τ_4 (inset picture) refers to the pore size.

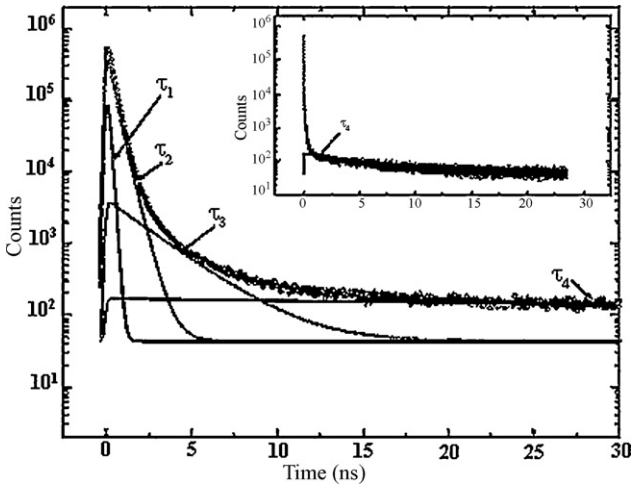

Fig. 4. Positron lifetime spectrum of sample 4. The spectrum consists of four lifetime components. The longest lifetime component τ_4 (inset picture) refers to the pore size.

Table 1 represents the positron and o-Ps lifetimes (τ_2, τ_3 and τ_4) and intensities (I_2, I_3 and I_4) for the investigated samples. It is found that with increasing the sample preparation time at 130 °C the lifetime τ_4 slightly increases to reach 111 ns for sample 6 and the intensity I_4 decreases to 4.7%. Whereas τ_4 is 93 ns for sample 2 with $I_4 = 5.8\%$. τ_2 and τ_3 decrease to reach 0.360 and 2.1 ns respectively for sample 6 while for sample 2 are 0.401 and 3.65 ns. All samples showed σ_2 and σ_3 of 0.100 and 0.144 ns respectively.

A model for estimation the hole size is used. It assumes pores with cylindrical diameter D and infinite length. A calibration curve represents the o-Ps lifetime as function of the pore size. It was calculated with this model. For the generation of the calibration curve "o-Ps lifetime vs. pore size D" we employed the routine EELViS[24] which is based on the extended Tao-Eldrup (ETE) model as published in Refs.[15,25]. For calculation we assumed that the pores form infinitely long cylinders with a diameter d, which corresponds then to the mean free path D in the pores, $D = d$. From measuring porous glasses with known pore sizes, the overlap parameter δ of the ETE model was determined to $\delta = 0.193$ nm[26] in agreement with the literature.[27] The calibration curve established on this way was used to calculate the pore diameter D from the corresponding o-Ps lifetime. The lower o-Ps1 corresponds to small (0.2–1.0 nm) holes which can be found in any amorphous material due to the structural disorder. The higher o-Ps2 comes from larger mesopores. The observed lifetime of 93–111 ns corresponds to a hole size of $D = 6.8$–11.5 nm (D – diameter or mean free path in cylindrical holes of infinite length).

4. Conclusion

In this work, we demonstrated that the complex structure of fine HAp agglomerates can be analyzed using PALS combined with XRD and SEM techniques to obtain a consistent picture of porous structures in fine-grained HAp. The SEM images do not show formation of well-crystallized particles of HAp, however XRD patterns show that HAp particles are crystalline with crystal size of about 7 nm evaluated from Scherrer equation. In the investigated HAp samples, open mesopores were found using positron annihilation lifetime spectroscopy (PALS). At low concentration of reactants, the pore size varies between 6.8 and 11.56 nm, dependent on the treatment time at 130 °C. PALS results suggested that agglomerates have a homogeneous distribution of nanopores where the distribution of nanopores is relatively narrow. Homogeneous and relatively narrow distribu-

tion of nanopores reveal that the dominant force in formation of pure HAp agglomerates is weak van der Waals. In conclusion, fine HAp grains obtained by hydrothermal method and spray drying can be considered as an agglomerates of nanoparticles in the sense that they have a highly nanoporous structure having a pore size distribution that shows relatively few fines as compared to agglomerates of nanoparticles.

References

1. Descamps M, Hornez JC, Leriche A. Manufacture of hydroxyapatite beads for medical applications. *J Eur Ceram Soc* 2009;**29**:369–75.
2. Andres-Vergks M, Fernhdez-Gonzilez C, Martinez-Gallego M. Hydrothermal synthesis of calcium deficient hydroxyapatites with controlled size and homogeneous morphology. *J Eur Ceram Soc* 1998;**18**:1245–50.
3. Rodriguez-Clemente R, López-Macipe A, Gómez-Morales J, Torrent-Burgués J, Castaño VM. Hydroxyapatite precipitation: a case of nucleation–aggregation–agglomeration–growth mechanism. *J Eur Ceram Soc* 1998;**18**:1351–6.
4. Vasylkiv OO, Sakka Y, Skorokhod VV. Nanostructured materials: features of preparing nano-size powders of tetragonal zirconium dioxide stabilized with yittrium. *Powder Metall Met C+* 2005;**44**:228–39.
5. Kim DW, Oh SG. Agglomeration behavior of chromia nanoparticles prepared by amorphous complex method using chelating effect of citric acid. *Mater Lett* 2005;**59**:976–80.
6. Peglow M, Kumar J, Warnecke G, Heinrich S, Mörl L. A new technique to determine rate constants for growth and agglomeration with size and time-dependent nuclei formation. *Chem Eng Sci* 2006;**61**:282–92.
7. Wengeler R, Nirschl H. Turbulent hydrodynamic stress induced dispersion and fragmentation of nanoscale agglomerates. *J Colloid Interface Sci* 2007;**306**:262–73.
8. Vasylkiv O, Sakka Y, Skorokhod VV. Nano-explosion synthesis of multicomponent ceramic nano-composites. *J Eur Ceram Soc* 2007;**27**:585–92.
9. Yao W, Guangsheng G, Fei W, Jun W. Fluidization and agglomerate structure of SiO_2 nanoparticles. *Powder Technol* 2002;**124**:152–9.
10. Gregg SJ, Sing KW. *Adsorption, surface area and porosity*. London: Academic Press; 1988.
11. Tsyurupa MP, Davankov VA. Porous structure of hypercrosslinked polystyrene: state-of-the-art mini-review. *React Funct Polym* 2006; **66**:768–79.
12. Staab TEM, Krause-Rehberg R, Kieback B. Review: positron annihilation in fine-grained materials and fine powders—an application to the sintering of metal powders. *J Mater Sci* 1999;**34**:3833–51.
13. Mogensen OE. *Positron annihilation in chemistry*. Heidelberg, New York: Springer-Verlag, Berlin; 1995.
14. Pethrik RA. Positron annihilation—a probe for nanoscale voids and free volume? *Prog Polym Sci* 1997;**22**:1–47.
15. Gidley DW, Frieze WE, Dull TL, Yee AF, Ryan ET, Ho HM. Positronium annihilation in mesoporous thin films. *Phys Rev B* 1999;**60**:R5157–5160.
16. Pietsch W. An interdisciplinary approach to size enlargement by agglomeration. *Powder Technol* 2003;**130**:8–13.
17. Tao SJ. Positronium annihilation in molecular substances. *J Chem Phys* 1972;**56**:5499.
18. Froeschke S, Kohler S, Weber AP, Kasper G. Impact fragmentation of nanoparticle agglomerates. *J Aerosol Sci* 2003;**34**:275–87.
19. Ito K, Nakanishi H, Ujihira Y. Extension of the equation for the annihilation lifetime of ortho-positronium at a cavity larger than 1 nm in radius. *J Phys Chem* 1999;**B103**:4555–8.
20. Thraenert S, Hassan EM, Enke D, Fuerst D, Krause-Rehberg R. Verifying the RTE model: ortho-positronium lifetime measurement on controlled pore glasses. *Phys Status solid C* 2007;**10**:3819–22.
21. Kansy J. *LT for Windows, Version 9.0*. Bankowa 12, PL-40-007 Katowice, Poland: Inst. of Phys. Chem. Of Metals, Silesian University; March 2002 (private communication).
22. JCPDS Card No. 00-09-0432, 1996.
23. Meyer JL, Eick JD, Naneollas GH, Johnson LN. A Scanning electron microscopic study of the growth of hydroxyapatite crystals. *Calcif Tissue Res* 1972;**10**:91–102.
24. Zaleski R. *Excited energy levels and various shapes (EELViS)*. pl. Marii Curie-sklodosliej 1, 20-031 Lublin, Poland: Maria Curie-Sklodowska University, Institute of Physics, Department of Nuclear Methods; 2007.
25. Goworek T, Ciesielski K, Jasińska B, Wawryszczuk J. Positronium in large voids. *Silicagel Chem Phys Lett* 1997;**272**:91–5.
26. Thränert S, Enke D, Dlubek G, Krause-Rehberg R. Positron lifetime spectroscopy on controlled pore glass porosimetry and pore size distribution. *Mater Sci Forum* 2009;**607**:169–72.
27. Ciesielski K, Dawidowicz AL, Goworek T, Jasińska B, Wawryszczuk J. Positronium lifetimes in porous Vycor glass. *Chem Phys Lett* 1998;**289**:41–5.